International Journal of Fluid Mechanics & Thermal Sciences
2026, Vol. 12, No. 2, pp. 24–31
https://doi.org/10.11648/j.ijfmts.20261202.11

SciencePG
Science Publishing Group

Research Article

Computational Analysis of Yield Stress Fluid Behavior over a Heated Surface-mounted Block with Temperature-dependent Viscosity

Subhasree Dutta*

Department of Basic Science and Humanities, University of Engineering and Management, Kolkata, India

Abstract

A numerical investigation of laminar viscoplastic flow past a heated square cylinder on a plane wall is presented using the Bingham and Casson models with Papanastasiou regularization. A two-step methodology first establishes fully developed channel flow at Re = 100, then uses it as inflow for the main problem at Re = 500. Effects of Bingham number (Bn = 0, 10, 30) on flow structure are examined. Results show progressive growth of unyielded zones (black regions) with increasing Bn, where fluid behaves as a rigid solid body. At Bn = 0, no unyielded zones exist, and symmetric streamlines with recirculation are observed. At Bn = 10, unyielded zones emerge upstream and, in the wake, suppressing vortex formation. At Bn = 30, these zones form an elongated rigid plug that eliminates recirculation. The regularized model captures yield surface evolution without numerical instability. Yield stress fundamentally governs flow morphology; unyielded regions grow and coalesce as Bn increases, reducing deformation and suppressing convective mixing with significant implications for heat transfer. Temperature-dependent viscosity is characterized by the Pearson number Pn, while the Casson number Ca represents the yield stress to viscous force ratio. This study aids design of thermal systems for heat exchangers, polymer processing, food sterilization, drilling operations, and biomedical devices.

Keywords

Viscoplastic Fluid, Bingham Model, Yield Stress, Unyielded Zone, Papanastasiou Regularization

1. Introduction

The study of viscoplastic fluid flow past bluff bodies has garnered significant attention in recent decades due to its widespread applications in industrial and engineering processes. Viscoplastic fluids, characterized by the presence of a yield stress, exhibit complex flow behaviour that differs fundamentally from Newtonian fluids. These fluids remain rigid when the applied stress is below a critical threshold, known as the yield stress, and flow only when this threshold is exceeded. Such behaviour is commonly observed in various materials including drilling muds, food products, slurries, polymer solutions, paints, cosmetics, and biological fluids such as blood [1, 2]. The comprehensive treatise by [1] laid the fundamental framework for understanding the dynamics of polymeric liquids, while [2] provided extensive insights into the behaviour of bubbles, drops, and particles in non-Newtonian fluids, establishing the foundational knowledge necessary for analyz-

*Correspondence: Subhasree Dutta (subhdutt050293@gmail.com)

Received: 2 April 2026; **Accepted:** 17 April 2026; **Published:** 21 May 2026

ing complex multiphase systems involving viscoplastic materials.

The flow past a square cylinder mounted on a plane wall represents a fundamental configuration that finds practical relevance in heat exchangers, electronic cooling systems, chemical processing equipment, nuclear reactors, and offshore structures. Understanding the flow dynamics around such bluff bodies is crucial for optimizing design parameters and ensuring operational efficiency. Early experimental investigations by [3] established the basic flow characteristics around bluff bodies, providing detailed insights into vortex dynamics, wake formation, and the transition from steady to unsteady flow regimes. Williamson's seminal work revealed the intricate relationship between Reynolds number and vortex shedding patterns, including the formation of Von Kármán vortex streets and the phenomenon of vortex dislocations. Subsequent numerical studies by [4] provided comprehensive insights into the wake dynamics and vortex shedding phenomena for Newtonian fluids, systematically examining the effects of Reynolds and Prandtl numbers on heat transfer characteristics from a square cylinder in the unsteady flow regime. Their work demonstrated that the flow undergoes a transition from steady to periodic at a critical Reynolds number, with significant implications for heat transport and drag forces.

The incorporation of non-Newtonian fluid properties adds considerable complexity to the flow physics, as the relationship between shear stress and strain rate becomes nonlinear and history dependent. [5] conducted comprehensive numerical simulations of Bingham plastic flow past a circular cylinder, demonstrating the formation of unyielded regions surrounding the obstacle. Their work revealed that increasing the yield stress leads to the enlargement of stagnant zones, significantly altering the flow field and drag characteristics. The study showed that for sufficiently high Bingham numbers, the unyielded regions attached to the cylinder surface grow and eventually merge, creating a solid-like envelope around the obstacle that dramatically changes the effective geometry experienced by the flowing fluid. Similarly, [6] investigated the creeping flow of Bingham plastics past a sphere, identifying the critical yield stress required to maintain unyielded regions. Their analysis provided valuable quantitative relationships between the Bingham number and the size and shape of unyielded zones, demonstrating that the drag coefficient increases monotonically with yield stress due to the expansion of rigid regions that effectively increase the obstacle size.

The Casson model, originally developed for blood flow applications [7], has been extensively employed to describe the rheological behaviour of viscoplastic materials with a yield stress. Casson's pioneering work provided a constitutive equation that accurately captures the shear-thinning behaviour accompanied by a yield stress, making it particularly suitable for suspensions and complex fluids such as printing inks, chocolate, and human blood. The model's mathematical structure, which involves a square root relationship between shear stress and shear rate, has been validated against numerous experimental datasets and remains widely used in biomedical and food engineering applications. [8] proposed an exponential regularization technique to overcome the numerical difficulties associated with the discontinuity at the yield surface, which arises from the singular behaviour of the apparent viscosity as the shear rate approaches zero. This innovative approach introduces a stress growth parameter that smooths the transition between yielded and unyielded regions, eliminating the need to track the yield surface explicitly while maintaining accuracy for sufficiently large values of the regularization parameter. This approach has been successfully implemented by various researchers [9, 10] to simulate viscoplastic flows across a wide range of Reynolds numbers. [9] applied the Papanastasiou regularization to study entry and exit flows of Bingham fluids in channels, demonstrating excellent agreement with analytical solutions and experimental observations. [10] provided some of the earliest numerical results for Bingham fluid flow in channels, establishing benchmark solutions that have been widely used for validation purposes.

The presence of thermal effects further complicates the flow dynamics, particularly when the fluid viscosity exhibits temperature dependency. Many industrial processes involving viscoplastic fluids operate under non-isothermal conditions, making the understanding of coupled flow and heat transfer essential for process design and optimization. [11] first addressed the thermal aspects of viscoplastic flows, developing theoretical frameworks for analyzing heat transfer in non-Newtonian systems and identifying the key dimensionless parameters that govern thermal transport. His work established that the yield stress significantly influences the temperature distribution and heat transfer rates by modifying the velocity profile and suppressing convective mixing. [12] provided a comprehensive review of heat transfer in non-Newtonian fluids, synthesizing decades of research and offering practical correlations for engineering calculations. The review covered forced, natural, and mixed convection regimes, as well as boiling and condensation phenomena in viscoplastic fluids. More recently, [13] investigated mixed convection from a heated cylinder in Bingham plastic fluids, highlighting the interplay between buoyancy forces and yield stress effects. Their study revealed that the Nusselt number exhibits complex behaviour as a function of Richardson number, with yield stress tending to suppress the enhancement in heat transfer typically associated with buoyancy-driven flows.

The flow of power-law fluids, which exhibit shear-thinning or shear-thickening behaviour without a yield stress, has also received considerable attention in the context of bluff body flows. [14] examined the flow of power-law fluids past a square cylinder, revealing that the shear-thinning behaviour leads to earlier vortex shedding and enhanced wake dynamics compared to Newtonian fluids. Their parametric study covered a wide range of power-law indices and Reynolds numbers, providing valuable insights into the role of non-Newtonian

viscosity on flow stability and drag. [15] considered the laminar flow and heat transfer characteristics for Newtonian fluids past a square cylinder in a channel, providing detailed benchmarks for validation of numerical methods and highlighting the effects of blockage ratio on flow development and thermal transport. Their work showed that confining walls significantly alter the wake structure and heat transfer rates compared to unconfined configurations, a finding that is particularly relevant for applications involving surface-mounted obstacles.

The fundamental concepts of plasticity and viscoplasticity were established in the early twentieth century. [16] introduced the foundational principles of fluidity and plasticity, providing the basis for understanding yield stress materials. [17] later formulated a rational description of the equations of plastic flow for a Bingham solid, formalizing the mathematical treatment of viscoplastic behaviour. Subsequent developments by [18] extended the regularization approach to three-dimensional Bingham plastic flows. [19] provided detailed analysis of viscoplastic flow past circular cylinders, identifying the conditions under which unyielded regions form and grow with increasing Bingham number. [20] further examined steady flow of Bingham plastics past square cylinders, demonstrating that the drag coefficient and wake length exhibit power-law dependence on the Bingham number in the high yield stress regime. [21] conducted detailed numerical simulations of heat transfer from a circular cylinder in Bingham plastic fluids, demonstrating that the local Nusselt number distribution is strongly influenced by the extent and location of unyielded regions around the cylinder. [22] investigated mixed convection heat transfer from a square cylinder in power-law fluids, demonstrating that the combined effects of buoyancy and shear-dependent viscosity produce complex heat transfer patterns that cannot be predicted by simple superposition of individual effects. [23] extended this analysis to square cylinders in Bingham plastic fluids, providing comprehensive data on drag coefficients and Nusselt numbers across a wide range of Reynolds and Bingham numbers. Their results showed that the critical Reynolds number for the onset of vortex shedding increases with Bingham number, and that heat transfer is significantly reduced in the presence of yield stress due to the suppression of recirculation and mixing. [24] examined steady flow of Bingham plastics past square cylinders, providing additional validation for numerical simulations. Finally, [25] proposed an alternative elasto-viscoplastic constitutive framework that combines yield stress behaviour with elastic effects.

Despite the substantial body of literature on viscoplastic flows, studies focusing on the combined effects of yield stress, temperature-dependent viscosity, and the presence of a surface-mounted obstacle remain limited. Most existing investigations consider idealized inflow conditions such as uniform velocity profiles or fully developed channel flows without addressing the coupling between flow development, obstacle geometry, and thermal transport. Previous investigations by [14] examined the flow of power-law fluids past a square cylinder, while [15] considered the heat transfer characteristics for Newtonian fluids in similar geometries. However, the comprehensive analysis of viscoplastic fluid flow past a heated square cylinder mounted on a plane wall, considering both Bingham and Casson constitutive models with temperature-dependent viscosity, has not been fully addressed in the literature. Furthermore, the influence of the Pearson number Pn, which characterizes the temperature dependency of viscosity, and the Casson number Ca, which represents the relative importance of yield stress to viscous forces, on the flow morphology and heat transfer characteristics remains largely unexplored for this configuration. The present study aims to fill this gap by developing a robust numerical framework that incorporates the Papanastasiou regularization technique, temperature-dependent viscosity, and realistic fully developed inflow conditions. The two-step methodology employed first establishes the fully developed velocity profile in a channel, which is then used as the inflow condition for the main problem of flow past a heated square obstacle mounted on a plane wall. The effects of key dimensionless parameters, including the Bingham number, Casson number, Reynolds number, and Pearson number, on the flow structure, unyielded zone evolution, and heat transfer characteristics are systematically investigated. The findings of this study are expected to provide valuable insights for the design and optimization of thermal systems involving viscoplastic fluids, with potential applications in heat exchangers, polymer processing, food sterilization, and biomedical devices.

2. Mathematical Model

The current investigation addresses this research gap by developing a robust computational methodology for analyzing laminar boundary-layer flow of viscoplastic fluids around a heated obstacle mounted on a flat surface. The key objectives are: (1) to formulate a two-step numerical approach for generating fully developed inlet conditions, (2) to examine the influence of yield stress parameters (Bingham number Bn and Casson number Ca) on the velocity field and yield surface morphology, (3) to assess the impact of temperature-dependent viscosity via the Pearson number Pn, and (4) to evaluate the predictive differences between the Bingham and Casson constitutive models under equivalent flow conditions.

The geometric arrangement, depicted in Figure 1, comprises a two-dimensional channel featuring a square-shaped protrusion of height H affixed to the bottom boundary. A uniform incoming flow at velocity U0 and cold temperature Tc enters through the inlet. The square obstacle is maintained at an elevated temperature Th > Tc, with its bottom face subjected to uniform heating ($\theta = 1$). The inlet is positioned 6H upstream of the obstacle, while the outlet is placed 13H downstream, allowing sufficient distance for the flow to achieve fully developed conditions before exiting. The domain height

is set to 10H, a dimension chosen to ensure negligible interaction between the top boundary and the flow structures developing around the obstacle.

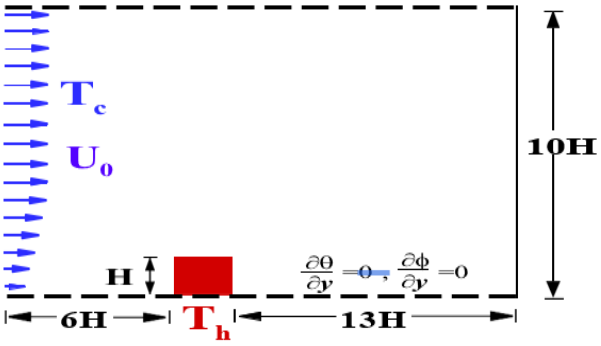

Figure 1. *Illustration of the geometric configuration depicting a square obstruction of height H positioned on a stationary wall. The computational region spans 6H upstream and 13H downstream of the obstacle, with a total vertical extent of 10H to minimize confinement effects.*

3. Boundary Conditions

A no-slip condition is enforced along the solid surface boundaries. The bottom face of the square obstacle experiences a uniform thermal condition (θ = 1). At the inlet boundary, the transverse velocity component is prescribed as zero.

$$u = U_0$$

Boundary Conditions:

at inlet: $u = U_0,\ v = 0,\ \theta = 0, \frac{\partial \phi}{\partial x} = -\left(\frac{1}{N_{BT}}\right).\frac{\partial \theta}{\partial x}$

at outlet: $\frac{\partial u}{\partial y} = 0, \frac{\partial v}{\partial x} = 0, \frac{\partial \theta}{\partial x} = 0, \frac{\partial \phi}{\partial x} = 0$

at bottom wall (non-obstacle): $u = 0,\ v = 0$

at top boundary (symmetry): $\frac{\partial u}{\partial y} = 0,\ v = 0$

at obstacle surface $\theta = 1$,

at fluid-solid interface:

$$\theta = \theta_s, \frac{\partial \theta}{\partial n} = Kr \left(\frac{\partial \theta}{\partial n}\right)_s$$

4. Fully Developed Flow of Non-newtonian Fluid

The non-dimensional form of the governing equations for the laminar boundary-layer flow of viscoplastic fluid are given by:

$$\nabla \cdot u = 0 \tag{1}$$

$$\left(\frac{\rho_{nf}}{\rho_f}\right)\left(\frac{\partial u}{\partial t} + u \cdot \nabla u\right) = -\left(\frac{\rho_{nf}}{\rho_f}\right)\nabla p + B\,\hat{e} + \left(\frac{1}{Re}\right)\nabla \cdot \left[\frac{\mu_{nf}}{\mu_f}\nabla u\right] + Ri\frac{(\rho\beta)_{nf}}{(\rho_f\,\beta_f)}\theta.e_g \tag{2}$$

$$\frac{(\rho Cp)_{nf}}{(\rho C_p)_f}\left(\frac{\partial \theta}{\partial t} + u \cdot \nabla\theta\right) = \frac{1}{Re\ .Pr}\nabla \cdot \left(\frac{k_{nf}}{k_f}\right)\nabla\theta + \frac{1}{Re.Pr\ .Le}\left(\nabla\theta \cdot \nabla\phi\right) + \frac{1}{Re\ .Pr\ .Le.N_{BT}}\left(\nabla\theta \cdot \nabla\theta\right) \tag{3}$$

$$\frac{\partial \phi}{\partial t} + u \cdot \nabla\phi = \frac{1}{Re.Sc}\nabla^2\phi + \frac{N_{BT}}{Re.Sc}\nabla^2\theta \tag{4}$$

Viscosity Modelling

Casson Model:

For viscoplastic fluids characterized by a yield stress, the Casson model establishes a relation- ship between the applied shear stress and the resulting deformation rate. The fundamental expression is given by:

$$\tau^{*\frac{1}{n}} = \tau_0^{*\frac{1}{n}} + \left(\mu_p\ \dot{\gamma}\right)^{\frac{1}{n}} \tag{5}$$

This can be rearranged to express the shear stress as:

$$\tau * = \left\{\left(\mu_p\right)^{\frac{1}{n}} + \left(\frac{\tau_0^*}{|\dot{\gamma}^*|}\right)^{\frac{1}{n}}\right\}^n \dot{\gamma}^* \text{ for } |\tau^*| > \tau_0^*, \tag{6}$$

while $\dot{\gamma}^* = 0$ when $|\tau^*| \leq \tau_0^*$.

The quantity τ_0^* represents the yield stress; its value being zero reduces the formulation to that of a Newtonian fluid. The parameter μ_p denotes the plastic viscosity, and the exponent n is conventionally taken as 2 for the standard Casson representation.

This formulation naturally partitions the flow domain into two distinct regions: a yielded zone where $|\tau^*| > \tau_0^*$, and an unyielded zone where $|\tau^*| \leq \tau_0^*$, with the interface between them referred to as the yield surface. As one approaches this interface, the shear rate $|\dot{\gamma}^*|$ approaches zero, leading to a singularity in the viscosity expression due to the presence of $\dot{\gamma}$ in the denominator. This behavior results in a discontinuity across the yield surface.

To overcome these computational challenges, an exponential regularization approach is adopted, following the method proposed by Papanastasiou. This technique introduces a stress growth parameter m that provides a smooth transition between the yielded and un- yielded regions through a single continuous function valid across the entire flow domain. The resulting Casson-Papanastasiou formulation takes the form:

$$\tau^* = \sqrt{\mu_p} + \frac{\tau_0^*}{|\dot{\gamma}^*|}\left(1 - e^{\{-m|\dot{\gamma}^*|\}}\right) \quad (7)$$

The plastic viscosity μ_p is modeled as temperature-dependent according to:

$$\mu_p(T) = \mu_p^0 \exp\{-b(T - T_c\}$$

Here, μ_0 represents the reference plastic viscosity constant, while b denotes the temperature- viscosity coefficient, which varies with the concentration of soluble solids in the fluid. Substituting this temperature dependence yields the generalized stress expression:

$$\tau^* = \left[\sqrt{\mu_p^0 \exp\{-b(T - T_c)\}} + \sqrt{\frac{\tau_0^*}{|\dot{\gamma}^*|}}\{1 - \exp(-m|\dot{\gamma}|)\}\right]^2 \dot{\gamma}$$

The non-dimensional form of the viscosity is defined as:

$$\mu_f = \left[\sqrt{\exp\{-P_n\theta\}} + \sqrt{\frac{Ca}{|\dot{\gamma}|}}\{1 - \exp(-M|\dot{\gamma}|)\}\right]^2 \quad (8)$$

In this expression, $Ca = \frac{\tau_0^* H}{\mu_p^0 U_0}$ represents the Casson number, which characterizes the relative importance of yield stress to viscous effects, while $P_n = b\Delta T$ denotes the Pearson number, capturing the temperature sensitivity of the viscosity. The present investigation considers only scenarios with positive values of P_n.

5. Fully Developed Velocity Profile in a Channel Flow

The contour plot of u-velocity and the downstream profile of u of the fully developed flow at the cross-section $x = x_0$ is provided below in Figure 2.

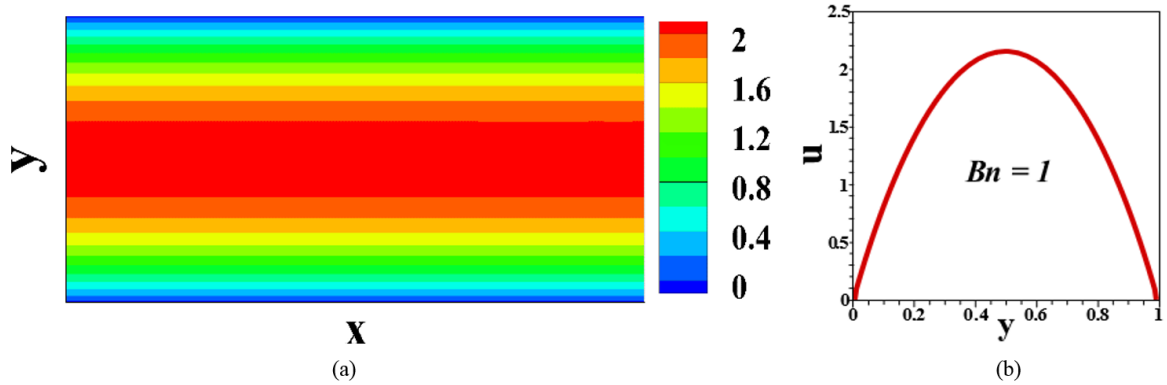

(a) (b)

Figure 2. *(a) Contour plot of u-velocity, (b) u-velocity profile along the channel cross section Re = 100.*

6. Fully Developed Velocity Profile for Unbounded Flow

The nonlinear second-order partial differential equations (1)-(6) are solved with appropriate boundary conditions specified. A uniform velocity u = 1 is considered at the inlet whereas no-slip boundary condition is taken at the wall of plate. The velocity profile u = u(y) obtained from the problem of uniform flow, is determined at some location $x = x_i$ so that the flow is fully developed.

The solution for the main problem of the viscoplastic fluid past as surface-mounted block is obtained by a two-step process. First, we determine the fully developed downstream flow as the solution of the predefined system at a point $x = x_0$, which is further used in the second step as the inflow velocity for the fluid flow around the solid heated obstacle mounted on the flat plate. Now we are continuing our work on this unbounded flow past a heated obstacle. Some results obtained for the flow field due to the variation of the yield stress parameter Bn based on Bingham model are provided below.

Effect of Yield Stress on Flow Structure and Unyielded Zones

The influence of yield stress on the flow morphology around the surface-mounted obstacle is examined through streamline visualizations and identification of unyielded regions. Figures 3-5 present the streamlines and the corresponding unyielded zones, highlighted in black, for three distinct Bingham numbers: Bn = 0, Bn = 10, and Bn = 30, at a fixed Reynolds number of Re = 500. The unyielded zones represent regions where the local shear stress remains below the yield

stress threshold ($|\tau| \leq \tau_0$), causing the viscoplastic fluid to behave as a rigid, solid-like body. Within these black regions, the fluid does not undergo internal deformation and instead translates as a cohesive plug, effectively acting as an extension of the solid obstacle.

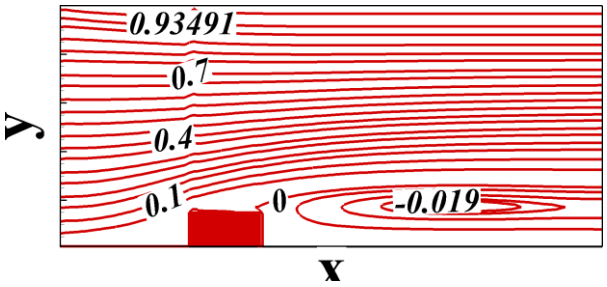

Figure 3. *Streamlines and corresponding unyielded zones (black regions) using the Bingham model for several Bingham numbers Bn =0 and Re = 500.*

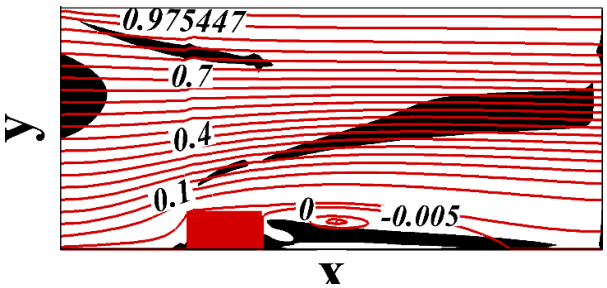

Figure 4. *Streamlines and corresponding unyielded zones (black regions) using the Bingham model for several Bingham numbers Bn =10 and Re = 500.*

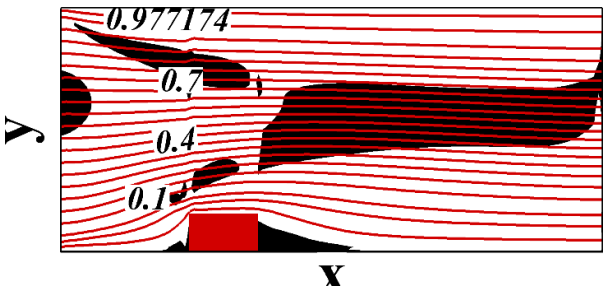

Figure 5. *Streamlines and corresponding unyielded zones (black regions) using the Bingham model for several Bingham numbers Bn =30 and Re = 500.*

For the limiting case of Bn = 0, the Bingham model reduces to a Newtonian fluid with no yield stress. Consequently, no unyielded zones are present in the flow domain, and the streamlines exhibit a symmetric pattern around the obstacle characterized by flow acceleration over the top surface of the block, a distinct recirculation region immediately downstream, and vortex shedding-like structures in the wake. In this case, the fluid yields everywhere, with continuous deformation throughout the domain.

As the Bingham number increases to Bn = 10, the introduction of yield stress significantly alters the flow topology, with the emergence of distinct unyielded zones in regions where the shear stress is insufficient to overcome the yield threshold. These black regions appear in two primary locations: a small unyielded zone forms directly in front of the obstacle where the fluid decelerates and shear stresses are minimal, and a more substantial unyielded zone develops in the immediate wake behind the obstacle. Within this downstream black region, the fluid moves as a rigid plug, effectively suppressing the formation of recirculation vortices that are typically present in Newtonian flows. The streamlines show a smoother transition around the obstacle with reduced curvature compared to the Newtonian case, indicating that a portion of the fluid behaves like a solid body, moving coherently without internal deformation and fundamentally altering the momentum transfer characteristics near the obstacle.

When the Bingham number is further increased to Bn = 30, the yield stress becomes sufficiently large to dominate the viscous forces over a significant portion of the flow domain. The unyielded zones expand considerably in both the upstream and downstream regions, with the black regions now occupying a substantial area behind the obstacle and creating an elongated rigid plug that extends far into the wake. This expanded unyielded zone effectively immobilizes the fluid in the recirculation region, completely suppressing vortex formation and wake unsteadiness. The streamlines for Bn = 30 exhibit a pronounced asymmetry and are forced to bypass a larger effective obstacle comprised of both the physical block and the surrounding unyielded rigid zones. The fluid yields primarily in the high-shear regions near the top corners of the obstacle and along the channel walls, while the core regions remain solid-like. This phenomenon, often referred to as the formation of a yield surface, highlights the self-amplifying nature of viscoplastic flow: regions of low shear stress become unyielded, which in turn alters the flow geometry and redistributes the stress field.

The evolution of unyielded zones with increasing Bn can be understood by considering the dimensionless yield stress parameter. When the local shear stress $|\tau|$ falls below the normalized yield stress Bn, the material cannot flow and instead translates as a rigid plug. As Bn increases, the criterion for yielding becomes more stringent, causing the unyielded regions to grow and coalesce. The black regions in Figures 3-5 thus represent zones where the viscoplastic fluid effectively acts as an extension of the solid obstacle, increasing the effective blockage ratio and altering the flow dynamics. This behavior has profound implications for heat transfer, as the solid-body motion within unyielded zones suppresses convective mixing and may lead to localized thermal stratification. The two-step numerical methodology employed in this study, which first establishes a fully developed inflow profile, successfully captures these complex yield surface evolutions, providing a robust framework for further investigation of coupled heat transfer phenomena in viscoplastic flows.

7. Conclusion

A numerical investigation of laminar viscoplastic flow past a heated surface-mounted obstacle was conducted using the Bingham and Casson constitutive models with Papanastasiou regularization, employing a two-step methodology wherein a fully developed flow profile was first established and subsequently used as the inflow condition for the main problem. The fully developed flow at Re = 100 yielded the classical parabolic velocity profile, validating the numerical implementation. Analysis of the flow structure at Re = 500 for Bingham numbers Bn = 0, 10, and 30 revealed the progressive growth of unyielded zones (black regions) with increasing yield stress. At Bn = 0, no unyielded zones were present, and symmetric streamlines with a distinct recirculation region were observed. At Bn = 10, unyielded zones emerged upstream and, in the wake, where the fluid behaved as a rigid solid body, suppressing vortex formation. At Bn = 30, these zones expanded significantly, forming an elongated rigid plug that extended far downstream and eliminated recirculation. The results demonstrate that the yield stress parameter fundamentally governs the flow morphology, as unyielded regions grow and coalesce with increasing Bn, reducing active deformation and suppressing convective mixing with significant implications for heat transfer. The regularized Bingham model successfully captured the yield surface evolution without numerical instability. Future work will extend this analysis to include temperature-dependent viscosity effects via the Pearson number Pn and explore the influence of the Casson number Ca on flow and heat transfer characteristics.

Abbreviations

B_n	Bingham Number, $\tau_0^* H/\eta U_0$
c_p	Specific Heat, $(Jkg^{-1}K^{-1})$
D_B	Brownian Diffusion Coefficient, $\frac{KBT}{3\pi\mu_f d_p}$
DT	Thermophoretic Diffusion Coefficient, $\frac{0.26(K_f\mu_f\ \phi_b)}{(K_p+2K_f)\rho f}$
g	Gravitational Acceleration, (m/s^2)
Gr	Grashof Number, $\frac{(1\ -\ \phi_b)(\beta_f g\Delta T H^3)}{\nu f^2}$
H	Enclosure Height, (m)
k	Thermal Conductivity, $\frac{W}{mK}$
Nr	Buoyancy Ratio, $\frac{\phi_b(\rho p_i\ -\ \rho_f)}{\{\rho_f\beta_f\Delta T\ (1\ -\ \phi_b)\}}$
Nu	Local Nusselt Number, $\left(\frac{knf}{kf}\right)\frac{\partial\theta}{\partial n}$
p^*	Pressure, $(\frac{N}{m2})$
Pr	Prandtl Number, $\frac{\nu_f}{\alpha_f}$
Re	Reynolds Number, $\frac{\rho_f U_0 H}{\mu_f}$
Ri	Richardson Number, $\frac{Gr}{Re^2}$
t^*	Time, (s)
t	Dimensionless Time
T	Temperature, (K)
(u, v)	Dimensionless Velocity Components in x, y Direction Respectively
$U0$ Greek symbols	Characteristic Velocity of the Flow, (m/s)
α	Thermal Diffusivity, (m^2/s)
β	Coefficient of Thermal Expansion
μ	Dynamic Viscosity, $(\frac{kg}{ms})$
ν	Kinematic Viscosity, (m^2/s)
θ	Dimensionless Temperature
ρ	Density, (kg/m^3)
ϕ Subscripts	Nanoparticles Volume Fraction
av	Average Value
b	Bulk Value
f	Clear Fluid
nf	Hybrid Nanofluid
p	Solid Particle
$*$	Dimensional Quantity
0	Clear Fluid ($\phi_b = 0$)

Author Contributions

Subhasree Dutta: Conceptualization, Methodology, Formal Analysis, Investigation, Visualization, Writing – original draft, Writing – review & editing

Conflicts of Interest

The author declares no conflicts of interest.

References

[1] Bird, R. B., Armstrong, R. C., & Hassager, O. (1987). Dynamics of polymeric liquids, Vol. 1: Fluid mechanics. John Wiley and Sons Inc., New York.

[2] Chhabra, R. P. (2006). Bubbles, drops, and particles in non-Newtonian fluids. CRC Press. https://doi.org/10.1201/9781420015386

[3] Williamson, C. H. K. (1996). Vortex dynamics in the cylinder wake. Annual Review of Fluid Mechanics, 28(1), 477-539. https://doi.org/10.1146/annurev.fl.28.010196.002401

[4] Sahu, A. K., Chhabra, R. P., & Eswaran, V. (2009). Effects of Reynolds and Prandtl numbers on heat transfer from a square cylinder in the unsteady flow regime. International Journal of Heat and Mass Transfer, 52(3-4), 839-850. https://doi.org/10.1016/j.ijheatmasstransfer.2008.07.035

[5] Mitsoulis, E. (2004). Effect of rheological properties on the drag coefficient for creeping flow around a sphere. Journal of Non-Newtonian Fluid Mechanics, 123(2-3), 191-200. https://doi.org/10.1016/j.jnnfm.2004.08.003

[6] Blackery, J., & Mitsoulis, E. (1993). Creeping flow of Bingham fluids around a sphere. Journal of Non-Newtonian Fluid Mechanics, 48(1-2), 101-114. https://doi.org/10.1016/0377-0257(93)80012-L

[7] Casson, N. (1959). A flow equation for pigment-oil suspensions of the printing ink type. Rheology of Disperse Systems, 84-102.

[8] Papanastasiou, T. C. (1987). Flows of materials with yield. Journal of Rheology, 31(5), 385-404. https://doi.org/10.1122/1.549926

[9] Abdali, S. S., Mitsoulis, E., & Markatos, N. C. (1992). Entry and exit flows of Bingham fluids. Journal of Rheology, 36(2), 389-408. https://doi.org/10.1122/1.550311

[10] O'Donovan, E. J., & Tanner, R. I. (1975). Some numerical results for the flow of a Bingham fluid in a channel. Journal of Non-Newtonian Fluid Mechanics, 1(2), 183-191. https://doi.org/10.1016/0377-0257(75)80013-4

[11] Turian, R. M. (1971). Thermal phenomena in non-Newtonian flow. AIChE Journal, 17(3), 607-614. https://doi.org/10.1002/aic.690170322

[12] Chhabra, R. P., & Richardson, J. F. (1999). Non-Newtonian flow in the process indus- tries. Butterworth-Heinemann.

[13] Nirmalkar, N., Chhabra, R. P., & Poole, R. J. (2013). Mixed convection from a heated circular cylinder in Bingham plastic fluids. International Journal of Heat and Mass Transfer, 66, 897-911. https://doi.org/10.1016/j.ijheatmasstransfer.2013.07.073

[14] Patil, P. M., & Kumar, P. (2012). Flow of power-law fluids past a square cylinder. Jour- nal of Non-Newtonian Fluid Mechanics, 169, 1-14. https://doi.org/10.1016/j.jnnfm.2011.12.001

[15] Sharma, N., & Eswaran, V. (2013). Laminar flow and heat transfer past a square cylinder in a channel. International Journal of Thermal Sciences, 64, 220-230. https://doi.org/10.1016/j.ijthermalsci.2012.09.009

[16] Bingham, E. C. (1922). Fluidity and plasticity. McGraw-Hill.

[17] Oldroyd, J. G. (1947). A rational formulation of the equations of plastic flow for a Bingham solid. Mathematical Proceedings of the Cambridge Philosophical Society, 43(1), 100-105. https://doi.org/10.1017/S0305004100023276

[18] Beverly, C. R., & Tanner, R. I. (1992). Numerical analysis of three-dimensional Bing- ham plastic flow. Journal of Non-Newtonian Fluid Mechanics, 42(1-2), 85-115. https://doi.org/10.1016/0377-0257(92)87003-M

[19] Volkov, P. K. (2000). Analysis of the flow of a viscoplastic fluid past a circular cylinder. Journal of Engineering Physics and Thermophysics, 73(2), 286-292. https://doi.org/10.1007/BF02681810

[20] Malik, M., & Sahu, A. K. (2007). Steady flow of a Bingham plastic fluid past a square cylinder. International Journal of Computational Fluid Dynamics, 21(8), 287-298. https://doi.org/10.1080/10618560701717068

[21] Chakraborty, J., Verma, N., & Chhabra, R. P. (2004). Numerical study of heat transfer from a circular cylinder in Bingham plastic fluids. International Journal of Heat and Fluid Flow, 25(5), 861-874. https://doi.org/10.1016/j.ijheatfluidflow.2004.04.004

[22] Liu, B. T., & Fan, J. R. (2011). Mixed convection heat transfer from a square cylinder in power-law fluids. International Journal of Heat and Mass Transfer, 54(15-16), 3555- 3563. https://doi.org/10.1016/j.ijheatmasstransfer.2011.03.049

[23] Prasad, A. K., & Chhabra, R. P. (2013). Forced convection heat transfer from a square cylinder in Bingham plastic fluids. International Journal of Thermal Sciences, 67, 156-171. https://doi.org/10.1016/j.ijthermalsci.2013.01.008

[24] Dazhi, Y., & Shaojun, L. (2006). Numerical simulation of viscoplastic fluid flow past a square cylinder. Journal of Hydrodynamics, 18(3), 312-317. https://doi.org/10.1016/S1001-6058(06)60069-4

[25] Saramito, P. (2001). A new constitutive equation for elastoviscoplastic fluid flows. Journal of Non-Newtonian Fluid Mechanics, 100(1-3), 27-41. https://doi.org/10.1016/S0377-0257(01)00178-1